

Constraints on galaxy formation from α -enhancement in luminous elliptical galaxies

D. Thomas,¹ L. Greggio^{1,2} and R. Bender¹

¹Universitäts-Sternwarte München, Scheinerstr. 1, D-81679 München, Germany

²Dipartimento di Astronomia, Università di Bologna, I40100 Bologna, Italy

arXiv:astro-ph/9809261v1 21 Sep 1998

8 November 2021

ABSTRACT

We explore the formation of α -enhanced and metal-rich stellar populations in the nuclei of luminous ellipticals under the assumption of two extreme galaxy formation scenarios based on hierarchical clustering, namely a *fast clumpy collapse* and the *merger of two spirals*. We investigate the parameter space of star formation time-scale, IMF slope, and stellar yields. In particular, the latter add a huge uncertainty in constraining time-scales and IMF slopes. We find that – for Thielemann, Nomoto & Hashimoto (1996) nucleosynthesis – in a *fast clumpy collapse* scenario an $[\alpha/\text{Fe}]$ overabundance of ~ 0.2 dex in the high metallicity stars can be achieved with a Salpeter IMF and star formation time-scales of the order 10^9 yr. The scenario of two *merging spirals* which are similar to our Galaxy, instead, fails to reproduce α -enhanced abundance ratios in the metal-rich stars, unless the IMF is flattened during the burst ignited by the merger. This result is independent of the burst time-scale. We suggest that abundance gradients give hints to distinguish between the two extreme formation scenarios considered in this paper.

Key words: galaxies: elliptical, formation scenario – α -enhancement – stellar populations – initial mass function

1 INTRODUCTION

An enhancement of α -elements* in the *metal-poor* stars of our Galaxy, with respect to the solar proportions, was first realized by Aller & Greenstein (1960), Wallerstein (1962) and Conti et al. (1967). Subsequent studies (see Truran & Burkert 1993; Gehren 1995, and references therein) have confirmed that the abundance ratios in metal-poor stars exhibit α/Fe larger than the solar ratios. Since α -elements are mainly produced in short-lived, massive stars, while a substantial contribution to Fe comes from Type Ia supernovae (SN Ia) with longer lived progenitors, this pattern is generally interpreted in terms of formation time-scales. In the early stages of the chemical evolution (i.e. at low metallicities) the stellar abundance ratios reflect the SN II products. As the metallicity in the interstellar medium (ISM) builds up towards the solar value, the $[\text{Mg}/\text{Fe}]$ ratio is significantly driven down by the products of SN Ia explosions (cf. McWilliam 1997 and references therein). Abundance ratios therefore carry information about the main contributors to the enrichment and the star formation time-scales (SFT).

In contrast to the Milky Way, it is generally impossi-

ble to resolve stars in elliptical galaxies, thus their chemical properties have to be inferred from spectral indices. Theoretical population synthesis models based on *solar* abundance ratios, while adequately describing the $\langle \text{Fe} \rangle$ -Mg₂ features observed in the low luminosity ellipticals, fail to reproduce these indices in brighter objects (Peletier 1989; Gorgas, Efstathiou & Aragón Salamanca 1990; Faber, Worthey & González 1992; Worthey, Faber & González 1992; Davies, Sadler & Peletier 1993). Specifically, at a given $\langle \text{Fe} \rangle$ index the Mg₂ index is stronger than predicted by such models. This result is usually interpreted in terms of an $[\text{Mg}/\text{Fe}]$ overabundance in the stellar populations inhabiting the most massive ellipticals. The following explanations for this α -enhancement have been proposed (e.g. Faber et al. 1992):

- (i) Short time-scales characterizing the process of formation of the stellar populations (SP) dominating the observed line indices.
- (ii) Selective mass loss, such that SN Ia products are lost more efficiently.
- (iii) An Initial Mass Function (IMF) biased towards massive stars.
- (iv) Lower rate of SN Ia with respect to what is appropriate for the Milky Way.

In cases (i) and (ii) the intracluster medium (ICM) should

* The so-called α -elements, i.e. O, Mg, Si, Ca, Ti, are build up by synthesizing ⁴He-particles.

be overabundant in iron, if the contribution of giant ellipticals (hereafter gEs) to the ICM pollution is large (Renzini et al. 1993). Recent results from ASCA indicate that the element ratios in the ICM are consistent with solar values (Mushotzky et al. 1996; Ishimaru & Arimoto 1997; Gibson, Loewenstein & Mushotzky 1997; Renzini 1997). This suggests that either gEs do not play a major role in establishing the ICM composition or options (i) and (ii) do not apply. Case (iv) is an ad hoc assumption without real justification. Observed nova rates and LMXB populations make it unlikely that early-type galaxies form less binary stars than later types (Davies 1996).

Options (i) and (iii) have been investigated numerically by several authors (Matteucci 1994; Tantalo et al. 1996; Vazdekis et al. 1996; Vazdekis et al. 1997; Gibson & Matteucci 1997; Chiosi et al. 1997) in the framework of monolithic collapse models for the galaxy formation. These models describe the elliptical galaxy as a single body, and their results are hence appropriate to describe the *global* properties of these objects. These studies concentrate on reproducing the trend of α -enhancement increasing with galactic mass, that can be inferred from the observed spectral indices. The main results of these computations are:

- (i) The classical wind models yield *decreasing* [Mg/Fe] overabundance with increasing galactic mass in contradiction to the observations.
- (ii) An increasing [Mg/Fe] with mass can be reproduced if the SFT becomes shorter with increasing mass of the elliptical. This is the case for the inverse wind models proposed by Matteucci (1994).
- (iii) Alternatively, an IMF getting flatter with increasing galactic mass reproduces the same pattern.

The most recent works on this subject tend to favour the flat IMF option for gEs (Vazdekis et al. 1997; Gibson & Matteucci 1997; Chiosi et al. 1997).

In this paper we re-investigate options (i) and (iii). Rather than addressing the question of the increasing overabundance with galactic mass, we seek under which conditions an overabundance at high Z – appropriate for nuclei of gEs – is produced. In doing so we consider a physically plausible scenario for the formation of giant ellipticals based on hierarchical clustering of CDM theory (White & Rees 1978; Frenk et al. 1985; Efstathiou et al. 1988).

Indeed there are several indications that merging must play an important role in galaxy formation. Approximately 50 per cent of luminous ellipticals host kinematically decoupled cores (Bender 1990; Bender 1996). In some cases, the SPs in these cores show markedly different properties in the spectral indices (Bender & Surma 1992; Davies et al. 1993). As shown by Greggio (1997, hereafter G97), the strong Mg₂ and $\langle \text{Fe} \rangle$ indices measured in the nuclei of gEs indicate a substantial degree of pre-enrichment in the gas which is converted into stars in the inner parts of these galaxies. Although not exclusively, this can be accomplished in a merging formation scenario, provided that gas dissipation plays an important role.

Kinematical properties and line strength features are then determined by the ratio of star formation and merging time-scales (Bender & Surma 1992; Bender, Burstein & Faber 1992). In this framework we can envisage two extreme cases for the formation scenario for ellipticals, mainly

distinguished by the overall formation time-scale of the object:

a) *Fast Clumpy Collapse*. On rather short time-scales (~ 1 Gyr), massive objects are built up by merging of smaller entities. Star formation (SF) occurs within these entities as they merge. The different dissipative properties of the newly formed stars and the gas produce a chemical separation, such that the enriched material flows to the centre (Bender & Surma 1992; G97). On a larger scale, however, the whole system participates in a general collapse, merging and SF occurring within the same (short) time-scale. We notice that, from a chemical evolution point of view, this formation mode can also be considered as a refinement of the classical Larson (1974) monolithic collapse.

b) *Merging Spirals*. The merging event occurs when the merging entities have already converted most of their gas into stars. For example, two spirals similar the Milky Way merge to form an elliptical galaxy (Farouki & Shapiro 1982; Negroponte & White 1983; Gerhard 1983; Barnes 1988; Hernquist 1993). Most of the stars in the merging entities have formed in a continuous and long lasting (~ 10 Gyr) SF process, leading to approximately solar abundances in the ISM. At merging, the (enriched) residual gas flows down to the centre (Hernquist & Barnes 1991; Barnes & Hernquist 1996) where it experiences a violent SF episode, with a short time-scale. The global formation process, however, lasts ~ 10 Gyr or more.

Semi-analytic models of galaxy formation in the framework of the CDM theory for structure formation (Kauffmann, White & Guiderdoni 1993; Lacey et al. 1993; Cole et al. 1994) provide a continuum between these two extremes, with a distribution of time-scales for the formation of ellipticals which depends on specific assumptions in the modeling. There are several arguments constraining short formation time-scales and old formation ages of elliptical galaxies, hence pointing towards the *fast clumpy collapse* model. They are mainly based on the tightness of Fundamental Plane relations, i.e. the relation between SPs and σ (Dressler et al. 1987; Djorgovski & Davis 1987) and the small scatter in M/L ratios perpendicular to the FP (Renzini & Ciotti 1993). Also the colour evolution (Aragón Salamanca et al. 1993), and the evolution of the Mg- σ relation with redshift (Bender, Ziegler & Bruzual 1996; Ziegler & Bender 1997) put the star formation ages of *cluster* ellipticals to high redshift ($z \gtrsim 2$). Despite this, the chemical outcome of scenario (b) is of interest, since we know that such mergers do occur (IRAS galaxies, e.g. Soifer et al. 1984; Joseph & Wright 1985; Sanders et al. 1988; Melnick & Mirabel 1990). If ellipticals in the field and in clusters are intrinsically different (e.g. Kauffmann, Charlot & White 1996), and those in clusters form earlier, and on shorter time-scales (Kauffmann 1996), the two distinct scenarios may be assigned to these two kinds of objects. We notice, however, that the α -enhancement does not seem to depend on cluster properties (Jørgensen, Franx & Kjærgaard 1995), at least within the errors. Also, the Mg- σ relation measured in many clusters is remarkably independent of the clusters properties (Colless et al. 1998). Finally, the Mg- σ relation for field ellipticals does not differ appreciably from that derived for the Coma Cluster (Bernardi et al., in preparation). Despite this, the observational situation is still far from being settled, and

we investigate on the predictions of both models to help in constraining the problem of the formation of ellipticals.

The paper is organized as follows. In Section 2 we provide a more detailed prescription of the theoretical model used in this paper. The results are presented and discussed in Section 3 and Section 4, respectively. The main conclusions are summarized in Section 5.

2 THE THEORETICAL MODEL

The basic constraints on our modeling, aimed to describe the SPs in the central parts of bright ellipticals, are:

- (i) Achieving high (super-solar) total metallicities (Z);
- (ii) Producing an α -enhancement of the order of $[\alpha/\text{Fe}] \sim 0.2\text{--}0.4$ dex, as implied by the observations.

The first requirement comes from the observed nuclear Mg_2 index and points towards either higher yields (i.e. shallow IMF) in the central regions or to a scenario of *enriched* inflow (Edmunds 1990, 1992; G97). The latter implies that the SPs inhabiting the nuclear regions of ellipticals are characterized by a metallicity distribution with a minimum metallicity $Z_m > 0$ (i.e. they are composite stellar populations, hereafter CSP). The second requirement, instead, comes from both Mg and Fe indices, thus in principle the two constraints might refer to different components of the CSP. However, since the Mg and Fe indices are measured in the same spectral range, the component of the CSP dominating the Mg_2 index also dominates the Fe index. **Hence, requirements (i) and (ii) must be met simultaneously from the SP dominating the visual light.**

The first constraint is accomplished with a high degree of chemical processing, hence a large fractional amount of gas has to be turned into stellar mass. This can be achieved either in short time-scales (perhaps like in galactic bulges) or long time-scales (as in galactic disks). The second characteristic points towards relatively short time-scales. Note that both constraints are generally more easily met when assuming a flatter IMF.

The *fast clumpy collapse* and the *merging spirals* modes differ mainly in their time-scales of the pre-enrichment processes. These are mimicked by assuming different initial conditions for the chemical processing of the gas which forms the CSP hosted in the central parts of the galaxy. In the *fast clumpy collapse* the process of formation is so fast that the galaxy can be viewed as a single body. Its chemical evolution can be described as a closed box with only radial separation of different SPs. The initial abundance for the SF process is assumed to be primordial. In the *merging spirals* model, instead, the gas which is turned into stars at the merging event has been enriched in the extended evolution history of the parent spirals leading to approximately solar abundances. The two different star formation histories are sketched in Fig. 1. The duration of the active SF process will be addressed to as the star formation time-scale τ_{SF} (arrows in the figure). In the case of the *merging spirals* model (bottom panel) the overall formation time-scale for the final elliptical is much longer than τ_{SF} . The phase of chemical enrichment in the parent spirals *before* the merger is indicated by the dashed line. The chemical outcome of this phase is reflected in the initial abundances assumed for the gas participating

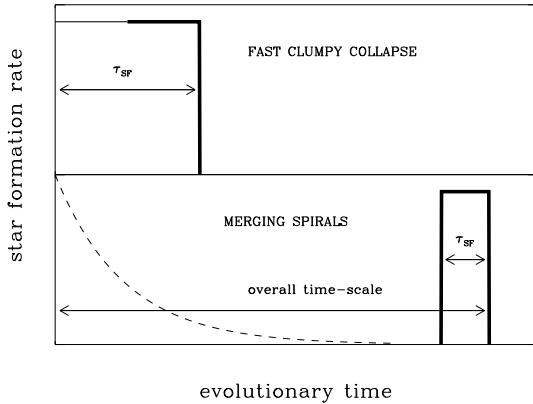


Figure 1. A sketch of the star formation histories assumed for the *fast clumpy collapse* (top panel) and the *merging spirals* (bottom panel) schemes. The arrows indicate the duration of the SF episode in the modeling (τ_{SF}). The thick solid lines indicate the SF episode yielding the SPs which end up in the central parts of the modeled galaxy. The dashed line (bottom panel only) sketches the rough star formation history of the parent spirals before the merger.

the merger (see Table 1). The thick lines in Fig. 1 indicate the metal-rich SPs that are assumed to form the nucleus of the object.

In the simulations, we consider a normalized mass of gas and calculate its chemical evolution until the gas is completely used up, yielding the maximum metallicity, which is appropriate for the most massive ellipticals. It should be noticed that in the models by Arimoto & Yoshii (1987) and Matteucci & Tornambè (1987) at the onset of the galactic wind the gas fraction is $0.01 - 0.05$ in the most massive models, depending on the IMF slope.

One further distinction between the two extreme cases for elliptical galaxy formation concerns the contribution of SNe Ia to the Fe enrichment of the high Z stars. In the merger of the two spirals we neglect the contribution from those SNe Ia whose progenitors were born in the parent spirals (dashed line in Fig. 1), and which explode after the merging. In other words, we assume that the products of these SNe Ia are not efficiently mixed down to the central part where the final burst occurs. This corresponds to maximizing the $[\text{Mg}/\text{Fe}]$ overabundance achieved in the nuclear CSP. In a *fast clumpy collapse*, instead, the merging entities are in close interaction, chemical mixing is likely to be more efficient. The model corresponds to the formation of the whole elliptical in a single event, and it seems quite artificial to exclude a fraction of the SN Ia products from the enrichment.

2.1 Input ingredients for the chemical evolution

We adopt a constant SFR in our computations, since in both models the SF episode generating the high Z stars has to be short to accomplish significant $[\text{Mg}/\text{Fe}]$ overabundances.

The chemical evolution is calculated by solving the usual set of differential equations as described in Thomas, Greggio & Bender (1998, hereafter Paper I). Enrichment due to planetary nebulae from low-mass stars (Renzini & Voli

1981), SNe II from high-mass stars (Woosley & Weaver 1995, hereafter WW95, and Thielemann, Nomoto & Hashimoto 1996, hereafter TNH96) and SNe Ia occurring in close binary systems (Nomoto, Thielemann & Yokoi 1984) are taken into account. The fraction A of close binaries is calibrated on a simultaneous fit of the age-metallicity relation in the solar neighbourhood and the ratio $N_{\text{Ia}}/N_{\text{II}} \approx 5$ typically observed in Sbc galaxies (van den Bergh & Tammann 1991), leading to $A = 0.035$ (see Paper I). The IMF is assumed as the usual single slope power-law normalized by mass, hence the slope $x = 1.35$ refers to the Salpeter value (Salpeter 1955). The upper and lower mass cut-offs are $40 M_{\odot}$ and $0.1 M_{\odot}$, respectively. The effect of adopting a different contribution from SN Ia, different mass cut-offs, and an IMF deviating from the single power law (e.g. Scalo 1986) are discussed below.

The time-scale τ_{SF} , and the IMF slope x represent the main parameters in the calculations.

2.2 Average abundances

The output of our models are abundances. For a comparison to the observational data the luminosity weighted average abundances have to be derived. The real abundances averaged by mass are larger, since at constant age metal-poor stars are brighter (e.g. G97). We shall compute both averages to figure out the effect quantitatively.

The mass averaged abundance of element i in a CSP of age t_g , including living stars and remnants, is given by the following eqn.:

$$\langle X_i \rangle_{*}(t_g) = \frac{\int_{t_0}^{t_1} X_i(t) \psi(t) m_*^{\text{SSP}}(t_g - t) dt}{\int_{t_0}^{t_1} \psi(t) m_*^{\text{SSP}}(t_g - t) dt}, \quad (1)$$

where t_0 and t_1 are respectively the epochs of start and end of the active SF process. The quantity $m_*^{\text{SSP}}(t_g - t)$ is the fraction of mass in stars (living and remnants) that, being born in t , are present at the epoch t_g (SSP means *Simple Stellar Population* of a fixed single age and single metallicity):

$$m_*^{\text{SSP}}(t_g - t) = \int_{m_{\min}}^{m_{\text{to}}(t_g - t)} \phi(m) dm + \int_{m_{\text{to}}(t_g - t)}^{m_{\max}} w_m \phi(m) dm \quad (2)$$

In Eqn. 2 m_{to} is the turn-off mass at epoch t_g of the SSP born at time t , m_{\min} and m_{\max} are respectively the lower and upper mass cut-offs of the IMF, and w_m is the remnant mass of a star of initial mass m . The values of w_m as a function of mass are taken from the nucleosynthesis prescriptions (see Paper I). As usual, the IMF $\phi(m)$ is normalized to 1. Thus the product $\psi(t) \times m_*^{\text{SSP}}(t_g - t)$ gives the mass contributed at the time t_g from the stellar generation born at epoch t , when the abundance in the ISM was $X_i(t)$.

In the light averaged abundance, the weights are given by the luminosity contributed at epoch t_g from the SSP born at time t :

$$\langle X_i \rangle_{\text{V}}(t_g) = \frac{\int_{t_0}^{t_1} X_i(t) \psi(t) L_{\text{V}}^{\text{SSP}}(t_g - t) dt}{\int_{t_0}^{t_1} \psi(t) L_{\text{V}}^{\text{SSP}}(t_g - t) dt} \quad (3)$$

where we have specified the V-band wavelength range because this is most relevant to our application. $L_{\text{V}}^{\text{SSP}}(t_g - t)$ is

Table 1. The initial abundances of the gas assumed to form the central stellar populations of the elliptical according to the merger of two spirals. The values for $0.5 Z_{\odot}$ are adopted from Paper I. The quantity τ_{pre} denotes the evolutionary time-scale of the parent spirals before the merger.

Z_{in}	τ_{pre}	[Fe/H] _{in}	[Mg/Fe] _{in}
$0.5 Z_{\odot}$	3 Gyr	-0.39	0.08
$1.0 Z_{\odot}$	10 Gyr	0.00	0.00

the luminosity at epoch t_g of an SSP of unitary mass with an age of $(t_g - t)$, and is given by SSP photometric models as a function of age and metallicity. In our application we will use the models by Worthey (1994). The spread in age and metallicity of the CSP are $[t_0, t_1]$ and $[Z_{\text{m}}(t_0), Z_{\text{M}}(t_1)]$, respectively.

The averaged abundance ratio is obtained by taking the ratio of the averaged abundances. For the sake of clarity, however, we use the following notation:

$$\langle [X_i/X_j] \rangle \equiv [\langle X_i \rangle / \langle X_j \rangle] \quad (4)$$

where the square brackets denote the usual normalization to the solar abundances, for which we use the meteoritic abundances given by Anders & Grevesse (1989).

3 RESULTS

In this section we present the results of our computations for the two extreme models of elliptical galaxy formation. In particular, we consider the average abundances 15 Gyr after the first episode of SF. However, since the passive evolution of SPs is most rapid in the first Gyr, the result is insensitive to the details of the star formation history and the exact age (Edmunds 1992).

Since most of the data in the literature concern magnesium and iron indices, we will concentrate on the average abundances of these two elements, thus on the possibility of producing an [Mg/Fe] overabundance. Mg can be considered as a representative for α -elements. Indeed, the ratios [Mg/Fe] and [O/Fe] do not differ significantly in the TNH96 models (Paper I). Also, we consider V-luminosity averaged quantities, since both the Mg and Fe indices fall in this spectral range.

In the following, we first discuss the average abundances for the closed box model. This is a good description of the *global* properties of an elliptical galaxy formed in a *fast clumpy collapse* mode. Second we look at the abundances of the high metallicity component of the closed box model. This is assumed to describe the properties of the *nuclear regions* of an elliptical galaxy formed in a *fast clumpy collapse* mode. Third we consider the *merging spirals* model in two possible initial conditions (see Table 1), corresponding to different degrees of enrichment of the ISM at the merging event, hence to different pre-enrichment time-scales.

The complete set of numbers for different parameter pairs of τ_{SF} , x , and Z_{m} and for both formation scenarios is presented in Table 2.

Table 2. The respective average stellar abundances (V-luminosity weighted) resulting from the *fast clumpy collapse* model (columns 4 – 7) and the *merging spirals* scheme (columns 8 – 10) for the different parameters IMF slope x , star formation time-scale, and minimum metallicity Z_m . TNH96 yields are adopted. In column 4, the quantity m_{CSP} denotes the mass fraction of the segregated composite stellar population for the *fast clumpy collapse*. In the *merging spiral* model, these fractions are determined by the fractions of gaseous mass when the merger occurs. The model for the evolution of the solar neighbourhood (Paper I) yields 0.5 and 0.2 for $Z_m = 0.5 Z_\odot$ and $Z_m = 1 Z_\odot$, respectively.

x	SFT (Gyr)	$Z_m (Z_\odot)$	m_{CSP}	FAST CLUMPY COLLAPSE			MERGING SPIRALS		
				$\langle [\text{Mg}/\text{Fe}] \rangle_V$	$\langle [\text{Fe}/\text{H}] \rangle_V$	$\langle [Z] \rangle_V$	$\langle [\text{Mg}/\text{Fe}] \rangle_V$	$\langle [\text{Fe}/\text{H}] \rangle_V$	$\langle [Z] \rangle_V$
1.35	0.3	0.0	1.0	0.27	-0.52	-0.27	–	–	–
		0.5	0.5	0.26	-0.20	0.03	0.18	-0.12	0.05
		1.0	0.2	0.25	-0.03	0.19	0.09	0.14	0.20
	1.0	0.0	1.0	0.20	-0.42	-0.22	–	–	–
		0.5	0.5	0.19	-0.12	0.06	0.15	-0.07	0.07
		1.0	0.3	0.18	0.03	0.20	0.07	0.18	0.23
	4.0	0.0	1.0	0.09	-0.24	-0.14	–	–	–
		0.5	0.6	0.07	-0.01	0.09	0.08	0.04	0.12
		1.0	0.3	0.06	0.17	0.22	0.04	0.23	0.29
1.00	0.3	0.0	1.0	0.34	-0.05	0.24	–	–	–
		0.5	0.8	0.34	0.11	0.38	0.28	0.17	0.39
		1.0	0.7	0.33	0.20	0.47	0.21	0.34	0.48
	1.0	0.0	1.0	0.28	0.07	0.31	–	–	–
		0.5	0.8	0.28	0.20	0.43	0.24	0.25	0.44
		1.0	0.7	0.28	0.29	0.50	0.19	0.41	0.53
	4.0	0.0	1.0	0.20	0.23	0.39	–	–	–
		0.5	0.8	0.20	0.34	0.48	0.18	0.38	0.50
		1.0	0.7	0.20	0.42	0.55	0.15	0.55	0.61
0.70	0.3	0.0	1.0	0.40	0.31	0.62	–	–	–
		0.5	0.9	0.40	0.40	0.70	0.36	0.44	0.70
		1.0	0.8	0.40	0.45	0.74	0.32	0.55	0.75
	1.0	0.0	1.0	0.35	0.45	0.70	–	–	–
		0.5	0.9	0.35	0.52	0.76	0.33	0.55	0.76
		1.0	0.9	0.35	0.56	0.79	0.29	0.65	0.81
	4.0	0.0	1.0	0.29	0.62	0.79	–	–	–
		0.5	0.9	0.29	0.67	0.83	0.27	0.70	0.84
		1.0	0.9	0.29	0.71	0.86	0.25	0.84	0.92

3.1 Predictions from the closed box model

As mentioned in the Introduction, an $[\text{Mg}/\text{Fe}]$ overabundance can be realized either with short SFTs or with a flat IMF. Correspondingly, different IMF slopes constrain differently this $\tau_{\text{SF}} \cdot x$ degeneracy, and consider two prescriptions for the SN II nucleosynthesis (WW95 and TNH96). In case of WW95 we adopt the results from model B which assumes an enhancement of the explosion energy in high mass stars by a factor 1.5 and therefore compares best to the TNH96 models. It should be noted that model B produces the highest $[\text{Mg}/\text{Fe}]$ ratio among the WW95 calculations (models A,B,C). For a detailed discussion we refer the reader to Paper I.

3.1.1 WW95 yields

Fig. 2 shows the averaged α -enhancement as a function of SFT and IMF slope for the WW95 stellar yields. The parameter range for τ_{SF} and x are chosen such that the resulting abundance ratios fall in the range indicated by the data (0.2 – 0.4 dex). As shown in Paper I, for these stellar yields the $[\text{Mg}/\text{Fe}]$ ratio in the SN II ejecta from one SSP is only slightly above solar. It follows that extremely short τ_{SF} are required to obtain values significantly above solar. In fact, Fig. 2 shows that a $\tau_{\text{SF}} \sim 10^7$ yr is necessary, irrespective of

the IMF slope. These results are presumably not compatible with the time-scale to cool the ejecta and to include them in the next generation of stars.

The minimum in $\langle [\text{Mg}/\text{Fe}] \rangle_V$ at $\tau_{\text{SF}} = 11 - 17$ Myr is a consequence of the metallicity dependence of the WW95 yields (included in our computations), in which the highest $[\text{Mg}/\text{Fe}]$ ratios are achieved for lowest ($10^{-4} Z_\odot$) and highest ($1 Z_\odot$) initial metallicity (see tables B1–B12 in Paper I). Thus in a regime where SPs of intermediate Z dominate the enrichment, the calculated overabundance reaches a minimum.

It should be noticed that the model for the SN Ia rate adopted in the computations does not influence this result. The Fe contribution from these objects starts to play a role only at ages larger than 10^8 yr. Lower Fe yields from SN II would lead to larger $\langle [\text{Mg}/\text{Fe}] \rangle_V$ for a given τ_{SF} . However, most of the Fe comes from stars of mass $\lesssim 20 M_\odot$ for which a lower Fe contribution would be unlikely (see Paper I).

In the model by Matteucci (1994) an α -element overabundance is still produced with SFTs of the order 10^8 yr. It is possible that the different results come from Matteucci (1994) having adopted Woosley (1986) yields which do not account for the fall back in high mass stars, and are therefore characterized by a huge magnesium yield from massive stars. We have shown in Paper I (Table 6) that an extrap-

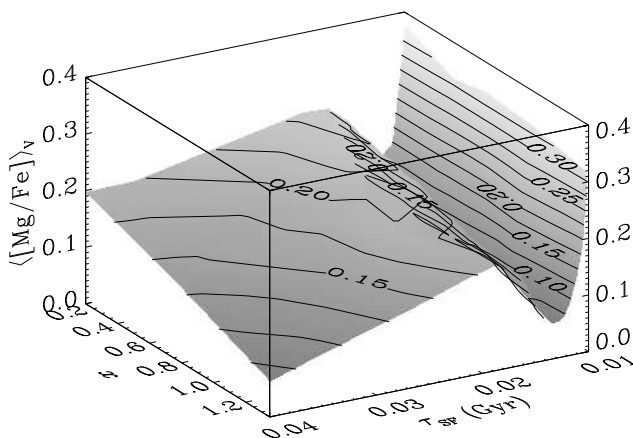


Figure 2. The figure shows the average $[\text{Mg}/\text{Fe}]$ overabundance in the stars weighted by V-band luminosity as a function of star formation time-scale and IMF slope (by mass). SN II nucleosynthesis is adopted from WW95. The contour lines mark the respective levels of constant $\langle [\text{Mg}/\text{Fe}] \rangle_V$. No segregation of metal-rich populations is considered, therefore the results are interpreted as *global* properties of the galaxy. The time-scales required for a significant α -enhancement are unplausible short ($\sim 10^7$ yr).

olation of the WW95 yields to the high mass end does not increase the Mg abundance in the ejecta of one SP significantly, again because of the fall back effect.

3.1.2 TNH96 yields

The results for TNH96 nucleosynthesis are presented in Fig. 3. In this case, τ_{SF} as long as a few Gyr still leads to an $[\text{Mg}/\text{Fe}]$ overabundance, provided that the IMF is not very steep. It is important to emphasize that the higher Mg yields in TNH96 basically stem from a higher contribution by stars in the intermediate mass range ($18 - 25 M_\odot$) which are not severely affected by fall back (Paper I). The results are more clearly illustrated in the 2-dimensional panels of Fig. 3, where we plot contours of constant $\langle [\text{Mg}/\text{Fe}] \rangle_V$, $\langle [\text{Fe}/\text{H}] \rangle_V$, and $\langle [\text{Z}] \rangle_V$ in the $\tau_{\text{SF}}-x$ -plane.

The average Z and $[\text{Fe}/\text{H}]$ are little sensitive to τ_{SF} , while they depend on the IMF slope. This is the mere consequence of having considered a closed box model which uses up all of the gas. In these cases the metallicity distributions extend up to the maximum possible value, which is given by the stellar yields of the SSP, and therefore only depends on the IMF slope, for a given stellar nucleosynthesis prescription. The contours are not totally flat because of the relaxation of the instantaneous recycling approximation which allows a delay in the enrichment. Since a substantial fraction of Fe comes from SN Ia the time dependence is larger for $\langle [\text{Fe}/\text{H}] \rangle_V$. The plots also show that the iron abundances are lower than the actual total metallicity by roughly $0.1 - 0.2$ dex. Hence at SFTs of the order one Gyr and below, Fe/H does not trace total metallicity Z very well.

From Fig. 3 one can see that $\langle [\text{Fe}/\text{H}] \rangle_V \approx 0$ is achieved with x in the range $1.2 - 0.9$. For these values of the IMF slope an $[\text{Mg}/\text{Fe}]$ overabundance of 0.25 is achieved with τ_{SF} in the range 0.8 to 2.6 Gyr. Restricting to the Salpeter's IMF ($x = 1.35$), one needs $\tau_{\text{SF}} \approx 0.1 - 1$ Gyr for an α -

enhancement in the range $\langle [\text{Mg}/\text{Fe}] \rangle_V \approx 0.2 - 0.3$ dex. The average iron abundance and metallicity, however, are low reaching $\langle [\text{Fe}/\text{H}] \rangle_V \approx -0.4$ and $\langle [\text{Z}] \rangle_V \approx -0.2$ for $\tau_{\text{SF}} \approx 1$ Gyr. The fact that the Salpeter IMF slope predicts sub-solar average metallicities should not be regarded as demanding flat IMFs for ellipticals. The observational constraints for super-solar metallicities (Davies et al. 1987; Worthey et al. 1992) concern the central parts of the galaxies, while the results discussed here refer to the global average metallicity of the galaxy. We will concentrate on this problem in the following subsections.

From now on we restrict our simulations to TNH96 nucleosynthesis, since, when adopting WW95 yields, the SF time-scales required to accomplish a $[\text{Mg}/\text{Fe}]$ overabundance seem unrealistically short.

3.2 Central abundances for the Clumpy Collapse model

In this model, the stellar populations dominating the central light of elliptical galaxies are those in the high metallicity tail of the closed box distribution. Since the chemical trajectory is characterized by decreasing overabundance as the metallicity increases, the larger the minimum metallicity (Z_m) adopted for the CSP inhabiting the central parts, the lower the average overabundance. This is demonstrated quantitatively in Fig. 4, where we show the predictions for our family of closed box models with Salpeter IMF (left-hand panel) and flat IMF with $x = 0.7$ (right-hand panel), and varying τ_{SF} . The dotted and dashed lines bracket the possible solutions, showing respectively the results for $Z_m = 0$ (no segregation of the high Z populations) and $Z_m = Z_M$, which is the highest Z attained by the closed box model ($Z_M \sim 3 Z_\odot$, $17 Z_\odot$ for $x = 1.35$ and $x = 0.7$, respectively). Adopting the Salpeter slope and $\tau_{\text{SF}} \lesssim 1$ Gyr a $\langle [\text{Mg}/\text{Fe}] \rangle_V \gtrsim 0.2$ dex is obtained for every choice of Z_m . The amount of iron locked in stars, instead, is much more sensitive to the segregation of the populations. In the case of $\tau_{\text{SF}} = 1$ Gyr when cutting the low-metallicity tail at $0.5 Z_\odot$, $\langle [\text{Fe}/\text{H}] \rangle_V$ increases from -0.44 to -0.15 dex. **For the super-solar populations in the centres of ellipticals, solar iron abundance ($\langle [\text{Fe}/\text{H}] \rangle_V = 0.01$), $[\text{Mg}/\text{Fe}]$ overabundance ($\langle [\text{Mg}/\text{Fe}] \rangle_V = 0.17$) and super-solar total metallicity ($\langle [\text{Z}] \rangle_V = 0.18$ dex) are achieved for Salpeter IMF with a star formation episode lasting 1 Gyr.**

The above example shows that a Salpeter IMF is compatible with the observations provided that τ_{SF} is shorter than ~ 1 Gyr. Longer τ_{SF} lead to overabundances that seem too small.

A flatter slope for the IMF obviously relieves the constraint on τ_{SF} . The case of $x = 0.7$ is shown in the right-hand panels of Fig. 4. One can see that τ_{SF} as long as 4 Gyr still yields an overabundance around 0.29 independent of Z_m . However, this slope tends also to yield very large $[\text{Fe}/\text{H}]$ values, which do not seem implied by the observations. Even with $Z_m = 0$ the average iron abundance is super-solar. It should be noticed that this is the consequence of the extremely large Z_M for this slope, i.e. $\approx 17 Z_\odot$. However, there are no known examples of stars with such high metallicities in any environment.

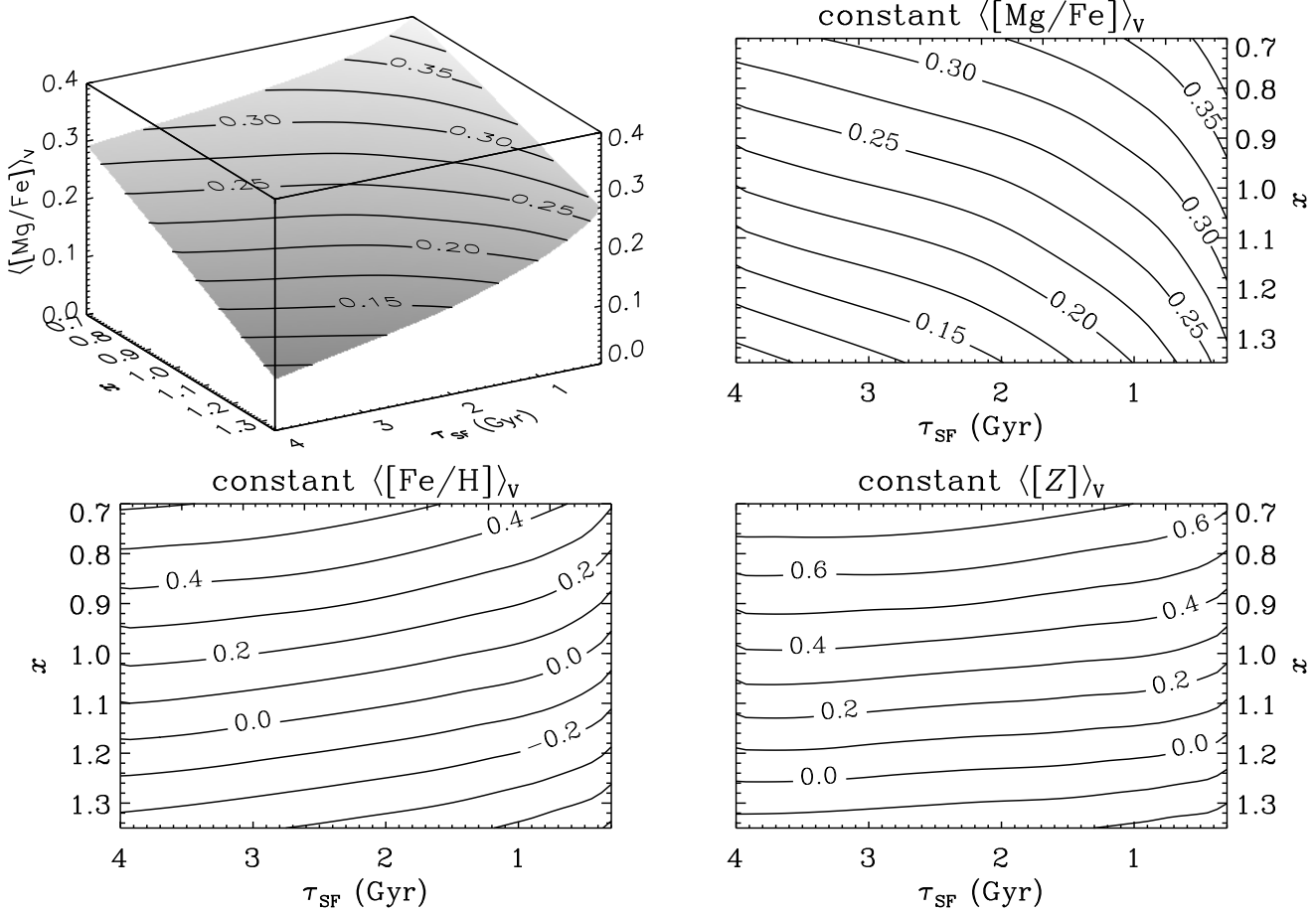


Figure 3. *Top-left panel:* The same as Fig. 2, however TNH96 nucleosynthesis is adopted. As a consequence, significantly longer star formation time-scales ($\lesssim 1$ Gyr) match the observed range of α -enhancement (0.2 – 0.4 dex). *Top-right panel:* A projection of the contours indicating constant $\langle [\text{Mg}/\text{Fe}] \rangle_V$ to the $\tau_{\text{SF}}-x$ -plane. *Bottom panels:* Contours of constant iron abundance (left-hand panel) and total metallicity (right-hand panel) are plotted as functions of τ_{SF} and x . The contours are not independent of τ_{SF} because finite stellar lifetimes are taken into account (Schaller et al. 1992). This effect is larger for iron due to the substantial contribution of SN Ia to the Fe enrichment. Generally, the total metallicity is larger than the iron abundance by 0.1 – 0.2 dex. The *global* values of both Fe/H and Z turn out to be *sub-solar* (–0.4 and –0.2 dex, respectively), if an [Mg/Fe] overabundance is accomplished with Salpeter IMF ($x = 1.35$).

Table 3. Mean stellar abundances (V-luminosity weighted) for the *fast clumpy collapse* model with $\tau_{\text{SF}} = 1$ Gyr, $x = 0.7$ and $Z_m = 0$, TNH96 yields. The fraction of gaseous mass transformed into stars is varied from $f_{\text{trans}} = 1.0$ (complete exhaustion) to $f_{\text{trans}} = 0.5$ to demonstrate the effect on the abundance ratios. The fifth column gives the total metallicity of the most metal-rich stars formed.

f_{trans}	$\langle [\text{Mg}/\text{Fe}] \rangle_V$	$\langle [\text{Fe}/\text{H}] \rangle_V$	$\langle [Z] \rangle_V$	Z_m
1.0	0.35	0.45	0.70	16.9
0.9	0.35	0.36	0.62	12.0
0.8	0.36	0.29	0.56	9.9
0.7	0.36	0.19	0.48	7.9
0.6	0.36	0.12	0.41	6.6
0.5	0.36	0.00	0.30	5.0

This ‘overproduction’ of metals can be compensated by transforming a smaller fraction f_{trans} into stars. Table 3 gives the results for various f_{trans} , and fixed $\tau = 1$ Gyr, $x = 0.7$, $Z_m = 0$. For this slope, in order to obtain $\langle [\text{Fe}/\text{H}] \rangle_V \lesssim 0.2$ dex (Worthey et al. 1992; Davies et al.

1993), less than approximately 70 per cent of the total gaseous mass should be converted into stars, with the rest being lost to the intergalactic or intracluster medium. Note that the most metal-rich population exhibits metallicities of $17 Z_\odot$ for the case of complete gas exhaustion.

3.2.1 Scalo-like IMF

Assuming an IMF which flattens out for $m \lesssim 0.5 M_\odot$ (Scalo 1986; Kroupa, Tout & Gilmore 1993; Gould, Bahcall & Flynn 1997) pushes more mass to massive stars and thus increases the efficiency of the chemical evolution processing. To investigate the effect on the results we performed additional simulations using the estimate of Gould et al. at the low-mass end

$$\begin{aligned} m < 0.6 M_\odot &\rightarrow \phi \sim m^{0.44} \\ 0.6 M_\odot \leq m \leq 1 M_\odot &\rightarrow \phi \sim m^{-1.21} \end{aligned}$$

and Salpeter slope above $1 M_\odot$. The averaged iron abundance – as compared to the single slope Salpeter case – is then further raised to $\langle [\text{Fe}/\text{H}] \rangle_V \approx -0.14$ dex, whereas the

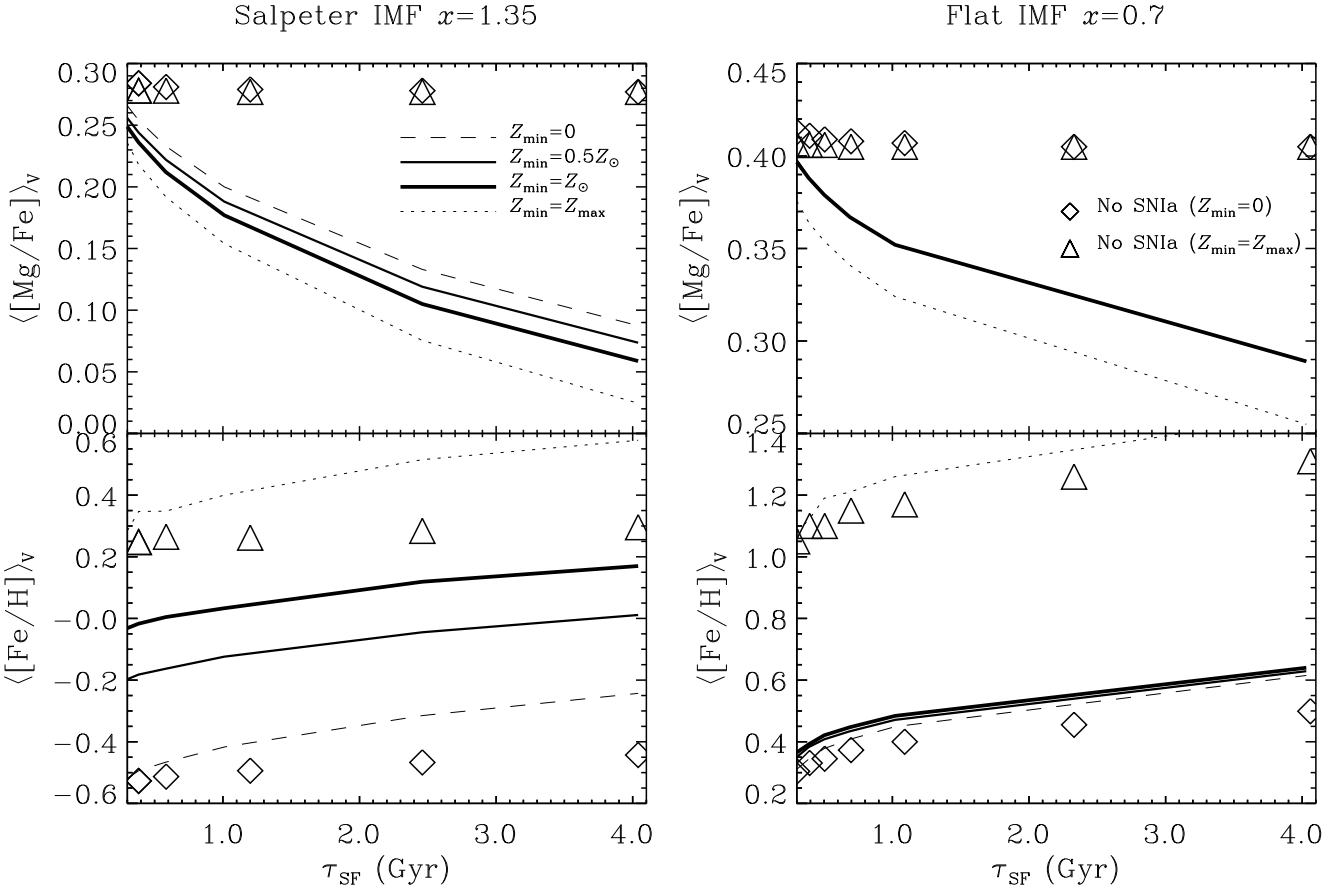


Figure 4. The figure shows the average stellar [Mg/Fe] overabundance (upper panels) and iron abundance (lower panels) in the *fast clumpy collapse* model as a function of star formation time-scale for Salpeter IMF (right-hand panel) and flat IMF (left-hand panel). TNH96 SN II yields are adopted. The various line-styles denote different minimum metallicities Z_m of the central stellar population. The symbols represent models excluding Type Ia supernovae for the two bracketing $Z_m = 0$ (diamonds) and $Z_m = Z_{\max}$ (triangles). The numbers are additionally shown in Table 2 (columns 4–7).

Mg/Fe ratio is not affected. Cutting the metal-rich part of the CSP at $Z_m = 1 Z_\odot$ leads to significantly super-solar abundances in iron ($\langle [Fe/H] \rangle_v \approx 0.18$ dex) and total metallicity ($\langle [Z] \rangle_v \approx 0.34$ dex).

If instead a steeper IMF $x = 1.7$ above $1 M_\odot$ is adopted (Scalo 1986), the iron abundance is slightly increased to $\langle [Fe/H] \rangle_v = -0.48$ dex. The degree of α -enhancement however, is reduced to $\langle [Mg/Fe] \rangle_v = 0.1$ dex. A Scalo slope of $x = 1.7$ at the high-mass end requires SFTs of the order 10^8 yr in order to produce $\langle [Mg/Fe] \rangle_v = 0.2$ dex. The reason for this pattern lies in the fact that apart from the contribution of SN Ia to the Fe enrichment, only high-mass stars above $8 M_\odot$ are responsible for the Mg/Fe ratio.

3.2.2 The SN Ia rate

The time-scales derived up to now are also dependent on the adopted description of the SN Ia rate (Greggio & Renzini 1983). In our models, each stellar generation gives rise to the first SN Ia event after 30 Myr from its birth, and 50% of the explosions occur within the first 0.5 Gyr approximately. We take this time as a characteristic time-scale for the Fe enrichment of the ISM from Type Ia explosions ($\tau_{Fe,Ia}$).

The level of the SN Ia rate has been calibrated on the chemical evolution of the solar neighborhood (Paper I). In our modeling, it yields a current rate of $R_{Ia} \approx 0.05 - 0.1 \text{ SNu}^\dagger$, depending on the IMF slope and the SFT. This result is in agreement with the lowest observational estimates of SNe Ia rates in ellipticals (see Cappellaro 1996, and references therein).

Given the uncertainties on the SN Ia progenitors, substantially longer $\tau_{Fe,Ia}$ could apply, and correspondingly an [Mg/Fe] overabundance could be accommodated with values of τ_{SF} systematically larger than derived in the previous section. We notice however that current models predict values of $\tau_{Fe,Ia}$ not significantly longer than ~ 1 Gyr (Greggio 1996). It is instructive to evaluate the possibility of suppressing completely the Fe contribution from SN Ia, since it also characterizes the assumption of selective mass loss (see options ii and iv in the Introduction). The results are shown in Fig. 4 as open symbols, where the diamonds refer to the av-

[†] $1\text{SNu} = 1\text{SN} \times (10^{10} L_\odot)^{-1} \times (100 \text{ yr})^{-1}$. The luminosities are taken from Worthey (1994).

eraged abundances of the total metallicity distribution, and the triangles to the abundances of the highest Z stellar population. Note that from stellar abundance ratios it is not possible to distinguish the options *selective mass loss* and *lower SN Ia rate*. For cluster ellipticals the ICM abundance in combination with the stellar abundances could be used to distinguish between the two options, under the assumption that gEs dominantly contribute to the ICM enrichment.

Without the Fe enrichment from SN Ia the $\langle [Mg/Fe] \rangle_v$ saturates at the maximum SN II-SSP value of 0.28 dex (Salpeter) and of 0.4 dex ($x = 0.7$), independent of the lower Z cut and the SFT, while $\langle [Fe/H] \rangle_v$ is shifted to lower values by roughly 0.2 dex. Total metallicity (not shown in the figure), instead, is lowered merely by 0.01 dex according to the small influence of SN Ia on Z for the SFTs considered here.

Both $[Mg/Fe]$ overabundance and iron abundance become virtually independent of τ_{SF} , since there is no delayed iron enrichment from SN Ia events. This computation trivially shows that without the SN Ia contribution, the α -elements overabundance does not constrain the SFT, while it constrains the SSP yields, and therefore, having chosen the nucleosynthesis prescriptions, the IMF slope. Adopting different models for the SN Ia progenitors with longer $\tau_{Fe,Ia}$, and/or assuming that a fraction of the Fe ejected by SN Ia is not incorporated in the ISM (i.e. selective mass loss) would lead to intermediate results. Accordingly, longer τ_{SF} , or steeper IMF slopes would meet the observational constraints. A quantitative exploration of the predictions of different SN Ia rates, with the appropriate calibrations on the solar neighborhood data and on the observed current rates, will be the subject of a forthcoming paper.

3.3 Central abundances in the model of merging spirals

As a second possibility for elliptical galaxy formation we consider the merger of two spirals, and discuss the chemical outcome from a star burst triggered by the merging event. The main difference with respect to the *fast clumpy collapse* case lies in the initial abundances adopted for the computation of the chemical evolution. Our model for the solar neighborhood (Paper I) predicts that a half solar and a solar metallicity are reached after 3 and 10 Gyr, respectively. We take the ISM abundances at these ages as initial conditions for the chemical evolution during the burst (see Table 1). We recall here that the model in Paper I adopts Salpeter IMF, which allows to reproduce the abundance patterns of the solar neighbourhood.

Modeling the burst of star formation we discuss the burst time-scale τ_{SF} , however the overall SFT of the object includes both τ_{SF} and the age of the parent spirals (see Fig. 1). For consistency, we look at the properties of the final galaxy at a total age of 15 Gyr, i.e. when the burst populations are 5 Gyr and 12 Gyr old in the cases of solar and half-solar pre-enrichment, respectively. Note, however, that the passive evolution of the SPs beyond 1 Gyr only provides a second order effect on the average abundances. The minimum metallicities of the populations formed at merging are by construction $Z_m = 0.5 Z_\odot$ and $1 Z_\odot$, and represent the stars in the galaxy core. The fractional amount of gaseous

mass is 50 per cent and 20 per cent for the $Z_{in} = 0.5 Z_\odot$ and $Z_{in} = 1 Z_\odot$ case, respectively.

The results of the calculations for the different parameters considered are summarized in the last two columns of Table 2, and plotted in Fig. 5, for Salpeter (left-hand panel) and flat IMF (right-hand panel). Again, the calculations neglecting SNe Ia are denoted by the symbols (diamonds: $Z_{in} = 1 Z_\odot$ and triangles: $Z_{in} = 0.5 Z_\odot$). For Salpeter IMF both models (solar and half-solar pre-enrichment) fail to produce at the same time high metallicity and $[Mg/Fe]$ overabundance. For half-solar initial abundances (characterized by an initial α -enhancement of 0.1 dex) the resulting average iron abundance is sub-solar. Starting with solar abundances, instead, super-solar iron abundance ($\langle [Fe/H] \rangle_v \approx 0.14$ dex) and metallicity ($\langle [Z] \rangle_v \approx 0.20$ dex) are achieved, whereas the $[Mg/Fe]$ overabundance ($\langle [Mg/Fe] \rangle_v \lesssim 0.1$ dex) is low. The apparently weak influence of neglecting SN Ia (symbols) comes from the fact that in this model SNe Ia are excluded only during the short burst phase. The iron provided by SN Ia explosions during the evolution of the parent spirals is included by construction in the initial conditions. Clearly, a flatter IMF during the burst yields a large overabundance, and high metallicities. It is worth noticing that the duration of the burst is not important with respect to the constraints considered here.

3.4 Comparison between the two models

We now turn to compare the results in the two extreme modes for the formation of elliptical galaxies. Inspection of Table 2 reveals that, for the same degree of pre-enrichment (i.e. Z_m):

- (i) The average metallicity $\langle [Z] \rangle_v$ of the central CSPs is approximately the same for the two models.
- (ii) The $\langle [Fe/H] \rangle_v$ is systematically larger, and the average $[Mg/Fe]$ overabundance is systematically lower, in the *merging spirals* model.

The first result simply reflects the fact that in both cases we have an overall closed box metallicity distribution with the same widths, the maximum metallicity being determined only by the nucleosynthesis prescriptions and the IMF slope. The second result is a consequence of the different initial conditions: in the *merging spiral* model all the Fe ejected by SN Ia during the past several Gyr of evolution of the parent spirals is incorporated in the gas undergoing the final burst of SF in the centre. In the *fast clumpy collapse* model, even the high metallicity stars form early, when pollution by SN Ia is still relatively modest. The larger α -enhancement achieved in this model is a direct consequence of the same effect. Indeed, the differences in both $\langle [Fe/H] \rangle_v$ and $\langle [Mg/Fe] \rangle_v$ are larger for the CSPs with $Z_m = 1 Z_\odot$, with respect to the cases with $Z_m = 0.5 Z_\odot$. When τ_{SF} is sufficiently long (e.g. 4 Gyr) the two models converge to similar results for $\langle [Fe/H] \rangle_v$ and $\langle [Mg/Fe] \rangle_v$, since in this case also in the *fast clumpy collapse* model most of the Fe ejected by SN Ia has been included in the high metallicity tail of the CSP.

4 DISCUSSION

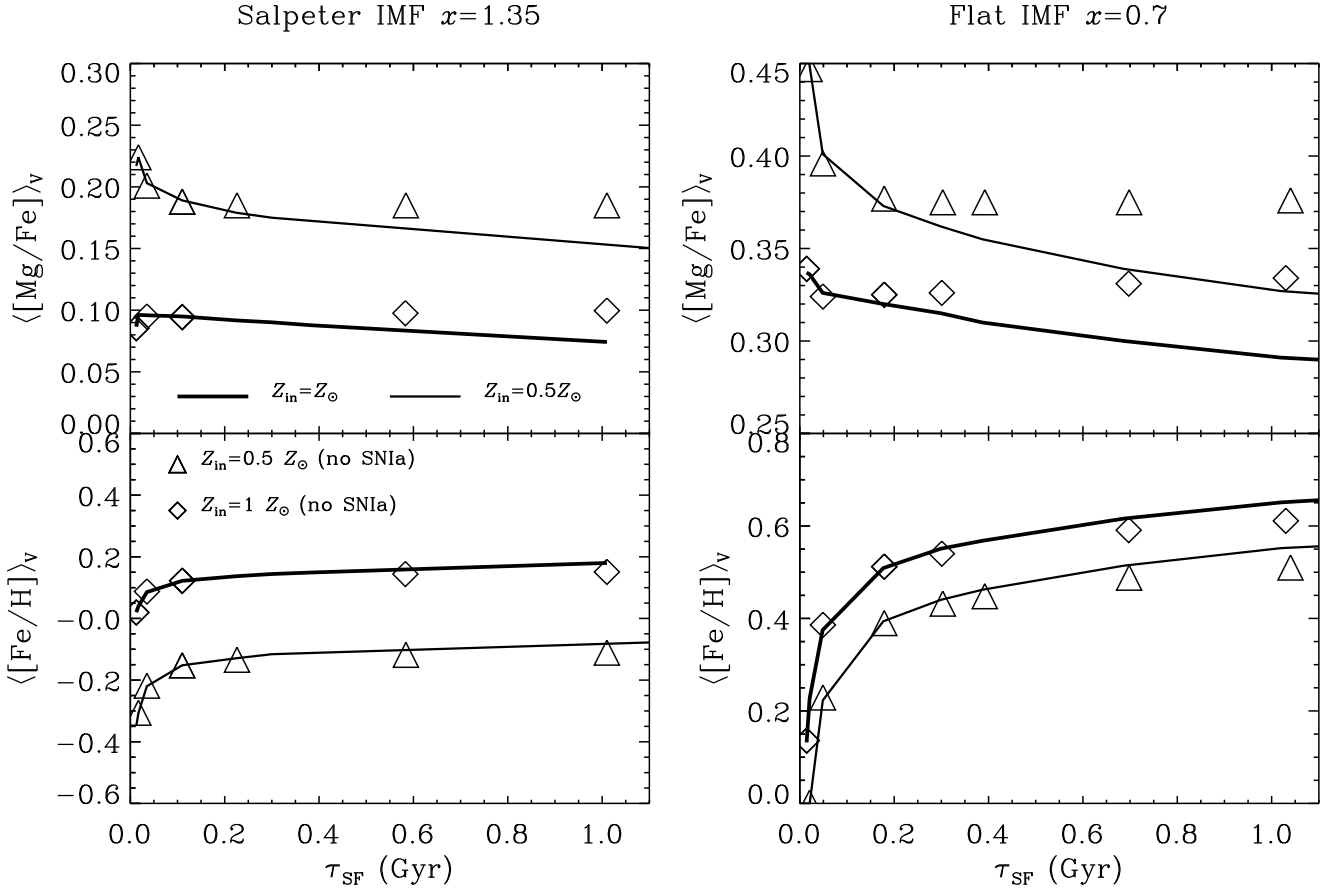


Figure 5. The figure shows the average stellar $[\text{Mg}/\text{Fe}]$ overabundance (upper panels) and iron abundance (lower panels) in the *merging spirals* model as a function of burst time-scale for Salpeter IMF (right-hand column) and flat IMF (left-hand column). TN96 SN II yields are adopted. The line-styles are the same as Fig. 4, denoting the respective degrees of pre-enrichment (see also Table 1). The symbols represent models excluding Type Ia supernovae *during the burst* for $Z_m = 0.5 Z_{\odot}$ (triangles) and $Z_m = 1 Z_{\odot}$ (diamonds). The numbers are additionally shown in Table 2 (columns 8–10).

4.1 Fast clumpy collapse vs. merging spirals

The two formation scenarios considered here can be distinguished by the time-scale on which the pre-enrichment of the central SPs to solar-like abundances is accomplished. In the *merging spirals* scenario, this time-scale is as long as several Gyr, and the pre-enriched gas that forms new stars has solar element abundances, in particular non α -enhanced abundance ratios. In the *fast clumpy collapse* scenario, instead, the pre-enriched gas forming the nucleus is overabundant in α -elements because of the preceding short SFT (shorter than 1 Gyr).

Our computations show that for the *clumpy collapse* both constraints for gEs, namely α -enhancement *and* super-solar metallicity, can be matched under the assumption of Salpeter IMF and SFTs up to 1 Gyr. High average metallicities are accomplished through segregating the metal-rich populations (with a minimum metallicity around $1 Z_{\odot}$) in the central region from the rest of the galaxy.

Super-solar *iron* abundance can be obtained if in addition a flattening of the IMF at the *low-mass end* around $0.5 M_{\odot}$ and Salpeter slope for masses above $1 M_{\odot}$ are ap-

plied. Flatter IMFs (in particular at the high mass end) generally allow longer SFTs, for the same $\langle [\text{Mg}/\text{Fe}] \rangle_v$, and lead to larger average metallicities. The metal ‘overproduction’ can be avoided by assuming that only a fraction of the initial gas mass is converted into stars, with consequences on the chemical enrichment of the intergalactic (or intra-cluster) medium. Besides, flatter IMFs, with metallicity distributions extending up to several times Z_{\odot} , do not require the segregation of the high metallicity SPs in the galaxy cores, to accomplish average metallicities in agreement with the observational indications. It is worth noticing, however, that there is no guarantee that these metallicity distributions would yield the strong Mg_2 indices observed in the central parts of the galaxies. In fact, the value of the indices depend on the *fitting functions* which seem to saturate at large metallicity (see G97).

In the case of merging of two Milky Way galaxies, the only way to achieve a high α -enhancement is to invoke a flat IMF in the final burst. This implies a large average metallicity for the central SP, with $\langle [Z] \rangle_v \approx 0.5$ already for $x=1$. In this case, it seems unlikely that the final burst does not proceed up to gas exhaustion, since the chemical process-

ing takes place deep in the potential well. Thus, if ellipticals form in this way, IMF slopes flatter than $x = 1$ seem highly unfavoured from the values of the Mg and Fe indices observed. The only way out would be to assume very short time-scales for the final burst of $\tau_{\text{burst}} \sim 10^7$ yr, which appears contrived. The merging of two spirals at early times in their chemical evolution looks more favourable, since our models starting from half solar initial conditions result in abundances marginally consistent with both observational constraints (α -enhancement *and* high metallicity).

4.2 Gradients inside the galaxy

In the *fast clumpy collapse* model, in order to accomplish large average metallicities in the core population we assumed a cut in the Z distribution, such that only stars with $Z > Z_m$ are found in the central parts of the galaxy. Correspondingly the low metallicity stars (Fig. 4) are in the outskirts, which qualitatively accounts for the observed metallicity gradients. As a consequence one expects that the stars in the outskirts of the elliptical galaxy should be more α -enhanced, with respect to those in the central parts, i.e. we expect a *positive* gradient in the [Mg/Fe] ratio. This pattern is present in the solar neighbourhood, with the metal-poor stars being more α -enhanced. In the merging spirals model, instead, the stars in the outer parts of the galaxy have approximately solar abundance ratios, i.e. ellipticals formed in this mode should exhibit *negative* gradients of [Mg/Fe].

Although the derivation of real abundances from line strengths measurements is highly uncertain (G97; Tantalo, Bressan & Chiosi 1997a, 1997b), so far the observations tend to indicate that the α -enhancement is either constant, or mildly decreasing from the centre to the outer parts of the ellipticals (Davies et al. 1993; Mehlert 1998). A trend of increasing overabundance with increasing metallicity (with a constant IMF slope) can only be achieved in a scenario in which the formation of the metal-rich population is evolutionarily decoupled from the star formation episode which generated the low metallicity stars, as assumed in our model of the *merging spirals*. In principle, one could apply this same decoupling also to the *fast clumpy collapse* picture, assuming that the SN Ia products of the low Z stellar generation do not mix efficiently with the collapsing gas, and are preferentially lost to the IGM. However, this looks rather artificial, due to the very short time-scale over which the formation of the whole galaxy is accomplished. Anyway, the measurement of abundance gradients offers the opportunity to discriminate between these two formation scenarios. It is therefore very important to better understand how the line strengths map into real abundances, and to study the trend of [Mg/Fe] overabundance with radius in great detail and in many objects.

4.3 Caveats and limitations

4.3.1 Luminosity *vs.* mass average

It is usually argued that the difference between luminosity and mass average is negligible (Arimoto & Yoshii 1987; Matteucci 1994). The derived abundances given in this paper are all weighted by the light emitted in the V-band, the specific V-luminosities as functions of age and metallicity

are adopted from Worthey (1994). In agreement with estimates by Edmunds (1992), the metallicity averaged by mass turns out to be systematically higher by 0.1 dex for Salpeter IMF, independent of the SFT:

$$\Delta[\text{Fe}/\text{H}] \equiv \langle [\text{Fe}/\text{H}] \rangle_* - \langle [\text{Fe}/\text{H}] \rangle_V \approx 0.1 \text{ dex}$$

Following the argument by Arimoto & Yoshii (1987) this is due to metal-poor K giants dominating the light in the V-band (see also Edmunds 1990). The effect on the [Mg/Fe] overabundance is significantly smaller, i.e.:

$$\Delta[\text{Mg}/\text{Fe}] \equiv \langle [\text{Mg}/\text{Fe}] \rangle_* - \langle [\text{Mg}/\text{Fe}] \rangle_V \approx -0.01 \text{ dex}$$

A flattening of the IMF lessens the discrepancy between mass and light average, hence $\Delta[\text{Fe}/\text{H}] \approx 0.05$ dex. However Worthey (1994) provides models for Salpeter slope only, causing an inconsistency in our approach. Indeed, at large ages the stellar M/L_B ratios are affected by the IMF slope adopted (Maraston 1998). To check the influence on our results, we additionally performed simulations using SSP luminosities derived by Buzzoni (1989), who provides models also for flatter IMF slope. It turns out that a $\Delta[\text{Fe}/\text{H}] \approx 0.05$ dex for Salpeter IMF is further reduced to $\Delta[\text{Fe}/\text{H}] \approx 0.02$ dex with $x = 0.7$. We conclude that within an uncertainty of 0.1 dex for the metallicity the difference between mass and light average in fact provides a minor effect independent of the IMF slope.

4.3.2 Stellar Yields

Our conclusions are strongly affected by uncertainties of SN II nucleosynthesis (Paper I; Gibson 1997a, 1997b; Portinari, Chiosi & Bressan 1998). We analyse the consequence of this problem by initially considering two different SN II yields (WW95, TNH96), but most of the computations are performed with TNH96, since they give the better fit to the solar neighbourhood data (Paper I). However, since TNH96 underestimate the Mg/O ratio by roughly 10 per cent (Paper I), and since the oxygen yield is likely to be better determined, there is the possibility that the Mg stellar yield is underestimated in TNH96 models. This leaves room to further relax the constraints on τ_{SF} and/or to reconcile the α -enhancement in ellipticals with the local IMF.

In our computations we assume an upper mass cut-off of $40 M_\odot$ for both WW95 and TNH96 SN II yields. Increasing the upper mass cut-off to $70 M_\odot$, and interpolating between TNH96 yields for a $40 M_\odot$ model and the Nomoto et al. (1997) yields of a $70 M_\odot$ -star, leads to an increase of ~ 0.15 dex of the [Mg/Fe]-ratio in the SN II ejecta in the case of Salpeter IMF (Paper I). Again, this relieves the constraints on the short τ_{SF} for the *clumpy collapse model*, or on the IMF slope. In particular, for the case of solar pre-enriched gas (merging Milky Ways) we performed additional calculations including the $70 M_\odot$ contribution to the ISM enrichment. Indeed, for Salpeter IMF we now obtain $\langle [\text{Mg}/\text{Fe}] \rangle_V \approx 0.2$ dex for $\tau_{\text{SF}} = 0.3$ Gyr. However, the actual contribution to the ISM from stars more massive than $40 M_\odot$ is highly uncertain (Paper I), due to the fall-back effect (WW95). Anyway, if these stars contribute substantially to the ISM pollution, the discrepancy in the derived overabundance between the *fast collapse* and *merging spirals* models becomes larger than what is shown in Table 2. Thus,

the conclusion that these two extreme cases of galaxy formation scenarios lead to different abundance ratios is even reinforced.

5 CONCLUSION

We have explored how to achieve the observed α -enhancement in luminous ellipticals in the three-dimensional parameter space of star formation time-scale, IMF slope, and stellar nucleosynthesis. As anticipated in Paper I on the basis of SSP yields, we find that, using the stellar yields from WW95, the observed $\langle [\text{Mg}/\text{Fe}] \rangle_V$ are reproduced only with extremely short star formation time-scales (SFT) of the order 10^7 yr. Therefore most of the results presented here have been obtained using TNH96 models.

It turns out that the abundance ratio $\langle [\text{Fe}/\text{H}] \rangle_V$ underestimates the real total metallicity of the system by $0.1 - 0.3$ dex depending on the SFT and IMF slope. We also briefly explored the difference between (V-band) light and mass average metallicity, finding that the mass averaged $[\text{Fe}/\text{H}]$ abundance ratios are ≈ 0.1 dex larger than the V-luminosity averaged ones. The effect on $[\text{Mg}/\text{Fe}]$ is instead negligible.

We have considered two extreme modes of elliptical galaxy formation, the *fast clumpy collapse* and *merging spirals* modes. We find that in the *fast clumpy collapse* model $\langle [\text{Mg}/\text{Fe}] \rangle_V \approx 0.2$ dex (in the high metallicity SPs) is obtained with IMF slopes close to Salpeter, provided that the overall formation time-scale does not exceed 1 Gyr. For the *merging spirals* model, instead, a sizeable overabundance is achieved only by claiming a flat IMF for the burst forming the central population. This is due to the large Fe content of the ISM at the epoch of the burst. The earlier the merging takes place in the chemical evolutionary history of the parent spirals, the easier it is to accomplish the overabundance in the burst population. In general, galaxy formation time-scales exceeding a few Gyr do not provide $\langle [\alpha/\text{Fe}] \rangle_V$ ratios consistent with observations, unless a significant deviation from the local IMF is allowed.

The two extreme models tend to predict opposite trends for the α -enhancement gradient within the galaxy: the *fast clumpy collapse* leads preferentially to larger overabundances in the outskirts where the low Z stars are formed. For the *merging spirals* model we expect approximately solar ratios in the outer stellar populations. If the merging occurs relatively early in the chemical evolution of the parent spirals, a slight α -enhancement is expected also in the outer stellar populations. Thus the behaviour of $\langle [\text{Mg}/\text{Fe}] \rangle_V$ with radius can give important hints on the galaxy formation process. Kauffmann (1996) proposed an intrinsic difference between the formation of cluster and field ellipticals, due to the high density environment favouring shorter galaxy formation (total) time-scales. If field objects are formed in a later merging event with respect to cluster objects we expect that field ellipticals tend to exhibit lower α -enhancement and steeper α -enhancement gradients than cluster ellipticals.

6 ACKNOWLEDGMENTS

We would like to thank the referee, M. Edmunds, for very interesting comments on the first version of the paper. We further thank S. E. Woosley for interesting and enlightening discussions. This work was supported by the "Sonderforschungsbereich 375-95 für Astro-Teilchenphysik" of the Deutsche Forschungsgemeinschaft.

REFERENCES

Aller L. H., Greenstein J. L., 1960, *ApJS*, 5, 139
 Anders E., Grevesse N., 1989, *Geochim. Cosmochim. Acta*, 53, 197
 Aragón Salamanca A., Ellis R. S., Couch W. J., Carter D., 1993, *MNRAS*, 262, 764
 Arimoto N., Yoshii Y., 1987, *A&A*, 173, 23
 Barnes J. E., 1988, *ApJ*, 331, 699
 Barnes J. E., Hernquist L., 1996, *ApJ*, 471, 115
 Bender R., 1990, in Wielen R., ed, *Dynamics and Interactions of Galaxies*. Springer Verlag, Heidelberg, p. 232
 Bender R., 1996, in Bender R., Davies R. L., ed, *New Light on Galaxy Evolution*, IAU Symposium 171. Kluwer Academic Publishers, Dordrecht, p. 181
 Bender R., Surma P., 1992, *A&A*, 258, 250
 Bender R., Burstein D., Faber S. M., 1992, *ApJ*, 399, 462
 Bender R., Ziegler B. L., Bruzual G., 1996, *ApJ*, 463, L51
 Buzzoni A., 1989, *ApJS*, 71, 817
 Capellaro E., 1996, in Bender R., Davies R. L., ed, *New Light on Galaxy Evolution*, IAU Symposium 171. Kluwer Academic Publishers, Dordrecht, p. 81
 Chiosi C., Bressan A., Portinari L., Tantalo R., 1997, *A&A*, submitted, astro-ph/9708123
 Cole S., Aragón Salamanca A., Frenk C. S., Navarro J., Zepf S., 1994, *MNRAS*, 271, 781
 Colless M., Burstein D., Davies R. L., McMahan R. K., Saglia R. P., Wegner G., 1998, *MNRAS*, submitted
 Conti P. S., Greenstein J. L., Spinrad H., Wallerstein G., Vardya M. S., 1967, *ApJ*, 148, 105
 Davies R. L., 1996, in Bender R., Davies R. L., ed, *New Light on Galaxy Evolution*, IAU Symposium 171. Kluwer Academic Publishers, Dordrecht, p. 37
 Davies R. L., Burstein D., Dressler A., Faber S. M., Lynden-Bell D., Terlevich R. J., Wegner G., 1987, *ApJS*, 64, 581
 Davies R. L., Sadler E. M., Peletier R. F., 1993, *MNRAS*, 262, 650
 Djorgovski S., Davis M., 1987, *ApJ*, 313, 59
 Dressler A., Lynden-Bell D., Burstein D., Davies R. L., Faber S. M., Terlevich R. J., Wegner G., 1987, *ApJ*, 313, 42
 Edmunds M. G., 1990, *MNRAS*, 246, 678
 Edmunds M. G., 1992, in Edmunds M. G., Terlevich R., ed, *Elements and the Cosmos*. Cambridge University Press, Cambridge, p. 289
 Efstathiou G., Frenk C. S., White S. D. M., Davis M., 1988, *MNRAS*, 235, 7
 Faber S. M., Worthey G., González J. J., 1992, in Barbuy B., Renzini A., ed, *The stellar populations of galaxies*, IAU Symposium 149. Kluwer Academic Publishers, Dordrecht, p. 255
 Farouki R. T., Shapiro S., 1982, *ApJ*, 259, 103
 Frenk C. S., White S. D. M., Efstathiou G., Davis M., 1985, *Nat*, 317, 595
 Gehren T., 1995, in Hippelein H., Meisenheimer K., Röser H.-J., ed, *Galaxies in the Young Universe*. Springer, Heidelberg, p. 190
 Gerhard O. E., 1983, *MNRAS*, 202, 1159
 Gibson B. K., 1997a, *MNRAS*, 290, 471

Gibson B. K., 1997b, in Cosmic Chemical Evolution, IAU Symposium 187, Kyoto, Japan. Kluwer Academic Publishers, Dordrecht

Gibson B. K., Matteucci F., 1997, MNRAS, 291, L8

Gibson B. K., Loewenstein M., Mushotzky R. F., 1997, MNRAS, 290, 623

Gorgas J., Efstathiou G., Aragón Salamaca A., 1990, MNRAS, 245, 217

Gould A., Bahcall J. N., Flynn C., 1997, ApJ, 482, 913

Greggio L., 1996, in Kunth D., Guiderdoni B., Heydari-Malayeri M., Thuan T. X., ed, The interplay between massive star formation, the ISM and galaxy evolution. Editions Frontières, Gif-sur-Yvette Cedex-France, p. 89

Greggio L., 1997, MNRAS, 285, 151 (G97)

Greggio L., Renzini A., 1983, A&A, 118, 217

Hernquist L., 1993, ApJ, 409, 548

Hernquist L., Barnes J. E., 1991, Nat, 354, 210

Ishimaru Y., Arimoto N., 1997, PASJ, 49, 1

Jørgensen I., Franz M., Kjaergaard P., 1995, MNRAS, 276, 1341

Joseph R. D., Wright G. S., 1985, MNRAS, 214, 87

Kauffmann G., 1996, MNRAS, 281, 487

Kauffmann G., White S. D. M., Guiderdoni B., 1993, MNRAS, 264, 201

Kauffmann G., Charlot S., White S. D. M., 1996, MNRAS, 283, L117

Kroupa P., Tout C. A., Gilmore G., 1993, MNRAS, 262, 545

Larson R. B., 1974, MNRAS, 169, 229

Lacey C. G., Guiderdoni B., Rocca-Volmerange B., Silk J., 1993, ApJ, 402, 15

Maraston C., 1998, MNRAS, in press

Matteucci F., 1994, A&A, 288, 57

Matteucci F., Tornambè A., 1987, A&A, 185, 51

McWilliam A., 1997, ARA&A, 35, 503

McWilliam A., Rich R. M., 1994, ApJS, 91, 749

Mehlert D., 1998, Phd thesis, Ludwig-Maximilians Universität, München

Melnick J., Mirabel I. F., 1990, A&A, 231, L19

Mushotzky R., Loewenstein M., Arnaud K. A., Tamura T., Fukazawa Y., Matsushita K., Kikuchi K., Hatsukade I., 1996, ApJ, 466, 686

Negroponte J., White S. D. M., 1983, MNRAS, 205, 1009

Nomoto K., Thielemann F.-K., Yokoi K., 1984, ApJ, 286, 644

Nomoto K., Hashimoto M., Tsujimoto F.-K., Kishimoto N., Kubo Y., Nakasato N., 1997, Nucl. Phys. A, 616, 79c

Peletier R., 1989, Phd thesis, Rijksuniversiteit Groningen

Portinari L., Chiosi C., Bressan A., 1998, A&A, 334, 505

Renzini A., 1997, ApJ, 488, 35

Renzini A., Ciotti L., 1993, ApJ, 416, L49

Renzini A., Voli M., 1981, A&A, 94, 175

Renzini A., Ciotti L., D'Ercole A., Pellegrini S., 1993, ApJ, 419, 52

Salpeter E. E., 1955, ApJ, 121, 161

Sanders d. B., Soifer B. T., Elioas J. H., Madore B. F., Matthews K., Neugebauer G., Scoville N. Z., 1988, ApJ, 325, 74

Scalo J. M., 1986, Fundam. Cosmic Phys., 11, 1

Schaller G., Schaerer D., Meynet G., Maeder A., 1992, A&AS, 96, 269

Soifer B. T., et al. , 1984, ApJ, 278, L71

Tantalo R., Chiosi C., Bressan A., Fagotto F., 1996, A&A, 311, 361

Tantalo R., Bressan A., Chiosi C., 1997a, A&A, submitted, astro-ph/9705060

Tantalo R., Bressan A., Chiosi C., 1997b, A&A, submitted, astro-ph/9710101

Thielemann F.-K., Nomoto K., Hashimoto M., 1996, ApJ, 460, 408 (TNH96)

Thomas D., Greggio L., Bender R., 1998, MNRAS, 296, 119 (Paper I)

Truran J. W., Burkert A., 1993, in Hensler G., Theis C., Gallagher J., ed, Panchromatic View of Galaxies. Editions Frontières, Kiel, p. 389

van den Bergh S., Tammann G. A., 1991, ARA&A, 29, 363

Vazdekis A., Casuso E., Peletier R. F., Beckmann J. E., 1996, ApJS, 106, 307

Vazdekis A., Peletier R. F., Beckmann J. E., Casuso E., 1997, ApJS, 111, 203

Wallerstein G., 1962, ApJS, 6, 407

White S. D. M., Rees M. J., 1978, MNRAS, 183, 341

Woosley S. E., 1986, in Hauck B., Maeder A., ed, Nucleosynthesis and Chemical Evolution. Geneva Observatory, Geneva

Woosley S. E., Weaver T. A., 1995, ApJS, 101, 181 (WW95)

Worthey G., 1994, ApJS, 95, 107

Worthey G., Faber S. M., González J. J., 1992, ApJ, 398, 69

Ziegler B. L., Bender R., 1997, MNRAS, 291, 527